An introduction for machining researchers to measurement uncertainty sources in thermal images of metal cutting

Eric P. Whitenton

National Institute of Standards and Technology,
Gaithersburg, MD 20899-8223, USA
E-mail: Eric.Whitenton@Nist.Gov

Abstract: Thermal imaging yields valuable information which improves and verifies the accuracy of machining models. There are three main steps involved when measuring temperature distribution of the tool, workpiece, or chip during metal cutting; acquiring a thermal image, converting imaged temperature to apparent temperature, and converting apparent temperature to true temperature. There are many error sources to consider. It is important to understand how these error sources affect measurement uncertainty. Some are familiar to anyone performing thermography measurements, such as uncertainties in camera calibration. However, metal cutting presents unique measurement challenges due to factors such as the high magnification required, high surface speeds, micro blackbody effects, and changing emissivity.

This paper is an introduction, focusing on thermal images, though visible spectrum images are also shown. Some examples illustrate basic concepts, while others are more complex. For brevity, specifics of cutting experiments are not given, as this paper has a measurement focus.

Keywords: uncertainty; metal cutting; dual-spectrum; high-speed imaging; infrared thermography.

Reference to this paper should be made as follows: Whitenton, E.P. (xxxx) 'An introduction for machining researchers to measurement uncertainty sources in thermal images of metal cutting', *Int. J. Machining and Machinability of Materials*, Vol. X, No. Y, pp.000–000.

Biographical notes: Eric P. Whitenton is a General Engineer at National Institute of Standards and Technology (NIST) who has been performing high-speed thermal and visible spectrum imaging since 2002.

1 Introduction

This paper summarises, highlights and augments information from a freely available report (Whitenton, 2010b). See the report for details and additional references. Also, video clips illustrating the challenges of imaging machining are available (Whitenton, 2010a). The focus of this paper is on using thermal images to perform qualitative and quantitative temperature measurements of metal cutting. For brevity, specifics of the cutting experiments are not given, as this paper has a measurement focus. Other publications are available which focus on why temperature information is important (Ivester and Heigel, 2007), other temperature measurement techniques (Davies et al.,

2007; Longbottom and Lanham, 2005), and thermal imaging more generally (Holst, 2003; Zhang et al., 2010).

In general, the first time an important concept is discussed it is presented in italic. The symbol ≅ means 'corresponding to'. An introduction to the important terms and concepts will be presented next. This is followed by discussions of the three main steps involved when using thermal images to measure temperatures; acquiring a thermal image, converting imaged temperature to apparent temperature, and converting apparent temperature to true temperature.

2   Important terms and concepts

Thermal radiation is electromagnetic radiation emitted over a range of wavelengths by an object related to the object's temperature. The temperature of the object, along with other factors, determines the intensity at each wavelength. *Radiation thermography* is the use of a sensor to measure the thermal radiation emitted by an object, generally with the intent to determine the object's temperature. Sensors often contain only a single sensing element and yield a single measurement value. By contrast, a thermal camera uses a focal plane array (*FPA*), which is an array of sensors. By displaying the array of measured values, an image is formed which is a representation of the temperature distribution on the surface of the object. Each element of the array is a *pixel*. Each pixel corresponds to a location in space of the scene being imaged, called a *scenel*.

True temperature refers to the actual temperature of an object. *Apparent temperature* refers to the temperature reported by a 'perfect' camera, and includes properties of the scene being imaged such as emissivity and reflections. Note that this is not necessarily the same as the *imaged temperature*, which is the temperature reported by the actual camera, and also includes properties of the image acquisition process such as scattering in the camera optics.

It is important to remember that thermal cameras do not actually measure temperature. They measure intensity of electromagnetic radiation within a range of wavelengths during a period of time (the *integration time* of the camera). The calibration of the camera allows a user to convert these measured intensities to imaged temperatures. Imaged temperatures may be converted to apparent temperatures, and apparent temperatures may then be converted to true temperatures, if one has a qualitative and quantitative understanding of the physical properties of the objects, the characteristics of the camera, as well as the conditions encountered while acquiring the images. Attaining accurate true temperatures is generally the goal when using thermal cameras.

The wavelengths of light being detected depend on the spectral response of the camera and any filters used. It is common to use a filter to limit the spectral response to make the conversion from apparent temperature to true temperature easier. However, this requires much longer integration times to accommodate the decreased intensity, which increases motion blur. *Motion blur* occurs when the object in an image moves more than 1 pixel in that image during the integration time. For example, a small, stationary object, say only a few pixels in size, might appear as a dot in the image. However, if the object is not stationary and moves ten pixels during the integration time, the light from each location on the object will be distributed across ten pixels. This causes what looks like streaks which are ten pixels long. Since the light is distributed across ten pixels, the intensity often appears less bright than if all the light fell on just one pixel.

Spatial resolution may be thought of as either the size of the smallest object in space one can detect or as the smallest space between objects one can detect. Spatial resolution is affected by several factors. One factor is *scenel spacing*, the distance between scenels, since one cannot easily detect objects smaller than one scenel. Another factor, *optical resolution*, is determined primarily by the way light interacts with the optical system of the camera. Optical resolution is not accurately described by a single number, but as a curve such as a point spread function (*PSF*). There are several techniques available for measuring such curves (Baer, 2003; Boreman and Yang, 1995; Nill, 2001). One way of thinking of a PSF is to imagine the camera focused on a single point of light which would fill exactly one pixel of the FPA if the camera optics were perfect. In this case, the FPA would report the one bright pixel, with all neighbouring pixels having an intensity value of 0. Unfortunately, even when the image is in focus, real optics spread this point over an area. The curve describing how the light is spread is the PSF. The wavelength of light affects optical resolution; shorter wavelengths can resolve smaller features than longer wavelengths. Thus, all else being equal, the visible light camera will yield a sharper image than the thermal camera.

Temporal resolution is the shortest event in time one can detect. It is affected by both the integration time of the camera and the *frame rate* (the number of images acquired per unit time). *Intensity resolution* is the smallest change in light intensity one can detect. It is affected by factors such as noise in the FPA, and the fact that intensities are digitised and converted into digital levels, or *DLs*. *Field of view* is the width and height of the scene being imaged. *Depth of field* is the distance toward or away from the camera an object being imaged may move and still produce an acceptable image. Depth of field is dependent on the magnification used and the wavelength of light imaged.

A *blackbody* is an object or material that completely absorbs all incident radiation, and uniformly emits the maximum possible thermal radiation (is perfectly efficient) as described by Planck's Law. A body which is perfectly efficient in emitting thermal radiation is said to have an *emissivity* of one. Blackbodies with emissivities very close to one may be purchased and are used to calibrate thermal cameras. Most objects have an emissivity less than 1. Emissivity is an important characteristic of an object when converting apparent temperature into true temperature. For the same true temperature, the apparent temperature will increase with emissivity. Emissivity of the chip is very non-uniform and is dramatically different from the uncut metal due to changes in surface texture and to oxidation. In many cases, this is the single most difficult source of error to correct when measuring machining temperature. A *micro-blackbody* is a very small feature, such as a small deep hole or narrow deep crevasse, which has a very high emissivity. Machining chips often have micro-blackbodies. This contrasts with a properly conditioned cutting tool, which has relatively small changes in emissivity.

There are other considerations besides those mentioned above. Many published works exist describing thermal imaging in general, as well as procedures for converting intensities into true temperatures. For references and more detailed information, see the report (Whitenton, 2010b) upon which this paper is based. More information is also available on the web at Whitenton (2010a).

3   Acquiring a thermal image

3.1   *Examples of thermal images*

The examples presented were acquired using *MADMACS*, the MAnufacturing Deformation MACro videography System developed at NIST (Whitenton, 2010b). Figure 1 shows a schematic of MADMACS, which consists of a high-speed visible light camera, a medium-speed thermal camera, and a common primary lens so the two cameras are imaging the same scene. A cold mirror reflects visible light to the visible light camera and transmits thermal radiation to the thermal camera. Chilled, temperature controlled water is circulated to stabilise the temperatures of the optics. Through-the-lens lighting aids positioning of the camera system by projecting a spot of visible light onto the object being imaged. At an angle to the dual-spectrum system is a conventional camcorder which images the scene at a low magnification. A data acquisition system records timing information for the cameras, as well as other signals such as cutting forces. Software allows researchers to review the images and signals synchronised to each other. Figure 2 shows a schematic of a typical image output by the system during orthogonal cutting.

Figure 1   Dual-spectrum system used to measure machining processes (see online version for colours)
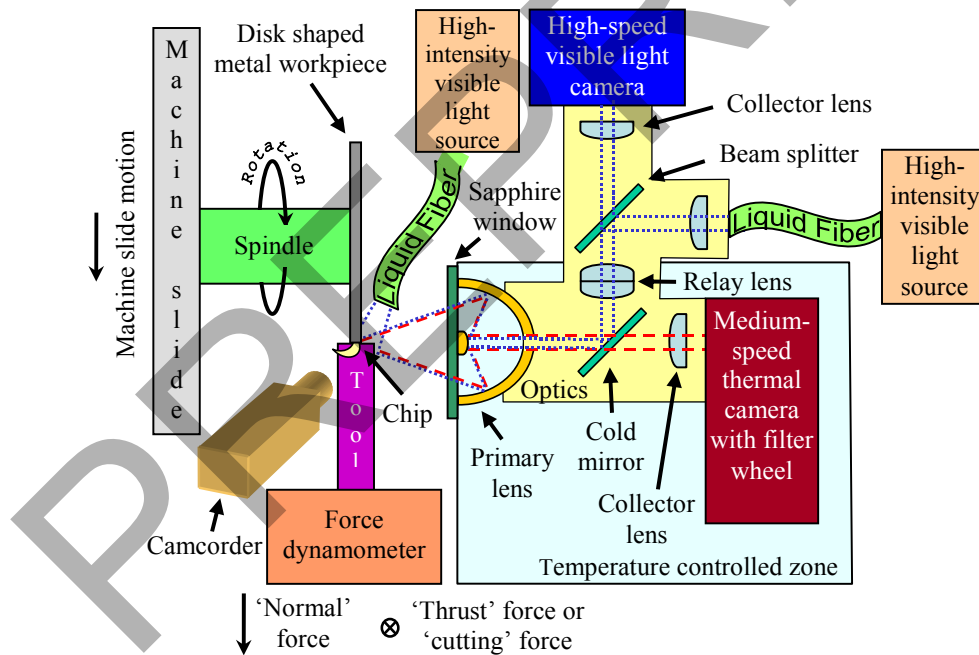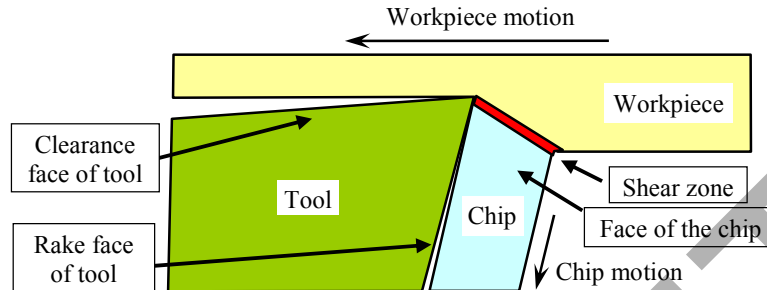
Figure 2   Schematic of an image of an orthogonal cutting process (see online version for colours)

A built up edge (*BUE*) is a lump of material which has built up on the cutting edge of the tool, forcing the chip to flow over it. Shown in Figure 3, the BUE can create a gap between the chip and the tool that can behave like a micro-blackbody. This causes this area of the image to have an emissivity very different from the emissivity of either the tool or the chip. If not taken into account, the higher than expected emissivity of the gap results in the derived true temperatures being positively biased (too high).

Figure 3   Image pairs from the dual-spectrum system
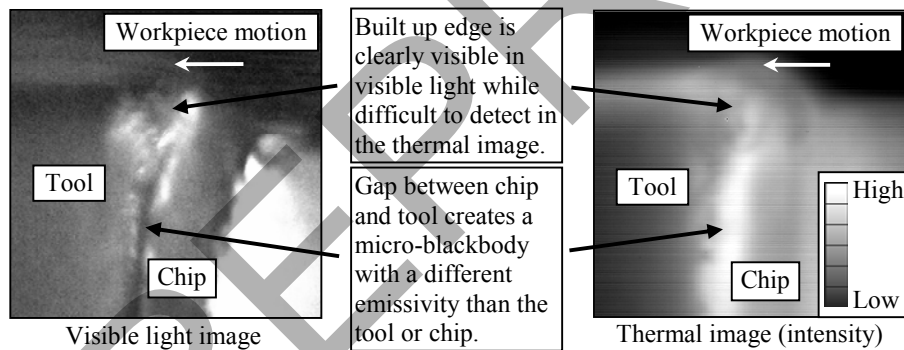
Note: Field of view is approximately 1 mm wide.

A *pig tail* occurs when a slender string of material flows out of the chip deformation zone towards the camera, perpendicular to the chip flow direction. The spiral shape of the material resembles a pig's tail. Pig tails move much slower than the chip, and often occur when the tool is worn. The visible/thermal image pair shown in Figure 4(a) shows a good imaged temperature measurement of the chip/tool interface. The presence of a pig tail is obvious in the central thermal image [Figure 4(b)], but not obvious in the lower thermal image [Figure 4(c)] without the accompanying visible light image. Since a pig tail moves at a much slower speed than the chip, the high frame rate of the visible light movies makes it easy to differentiate a pig tail from a chip. The speed at which an object moves is difficult to assess in thermal movies due to the relatively low frame rate of thermal movies. Note the 35°C difference between the top (good) and the bottom (aberrant) thermal images.

Figure 4   Pigtails, which adversely affect the accuracy of chip temperature measurements, are not always obvious in the thermal images. However, they are easily detected in the visible light images (see online version for colours)

(a)

(b)

(c)

Top view   Visible light image   Thermal image
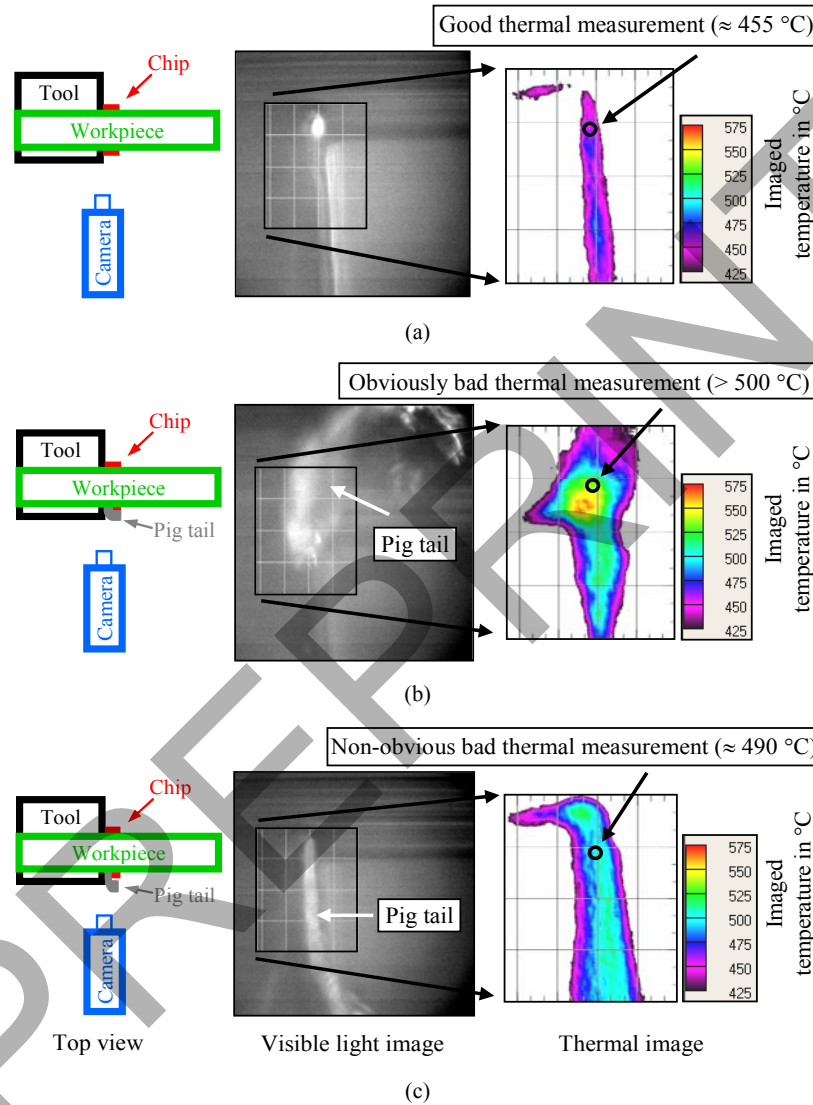
Notes: Field of view for the visible light images is approximately 2 mm wide. Field of view for the thermal images is approximately 1 mm wide.

Extraneous light sources must be considered and controlled to make accurate temperature measurements. The light entering a lens is not restricted to the light emanating from the field of view of the camera. Light from outside the field of view also enters the lens, and adds to the overall brightness level of the image due to reflections and scattering in the optical system. Shown in Figure 5, this may potentially affect both calibration and

imaging of machining. Figure 6 shows how light may also be reflected off of the surfaces being imaged, making them appear hotter than they actually are. The problem of extraneous light may be limited during calibration by placing an appropriately sized aperture between the camera and blackbody. During machining, one should be aware of the physical relationship in space between hot objects such as flying chips, the tool, and the workpiece.

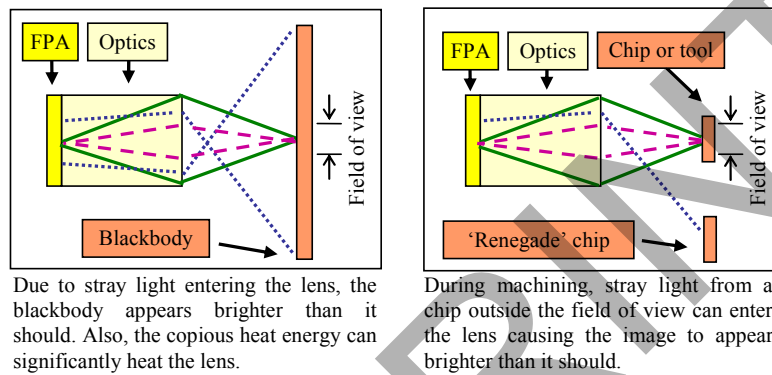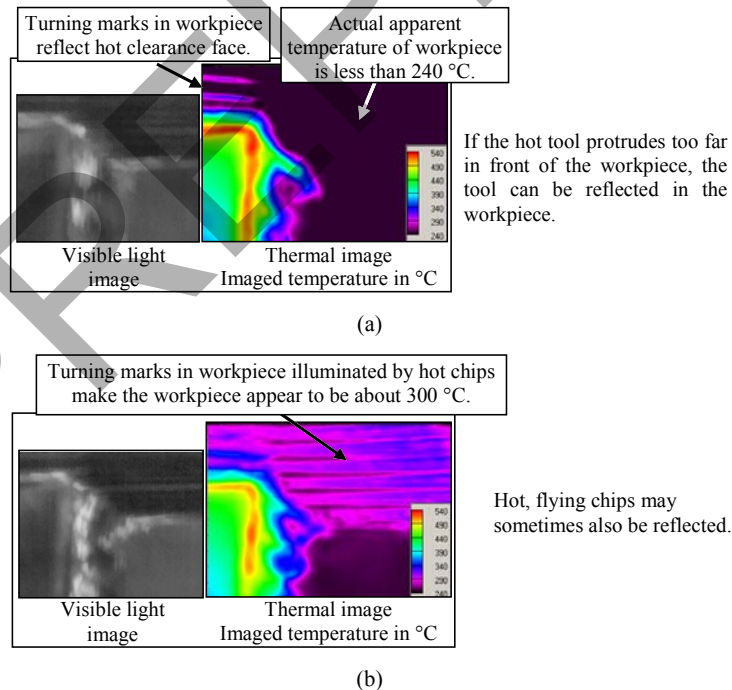**Figure 5**   Effects of stray light (see online version for colours)

Due to stray light entering the lens, the blackbody appears brighter than it should. Also, the copious heat energy can significantly heat the lens.

During machining, stray light from a chip outside the field of view can enter the lens causing the image to appear brighter than it should.

Figure 6   Two examples, acquired only milliseconds apart, of reflections affecting imaged temperature (see online version for colours)

Turning marks in workpiece reflect hot clearance face.

Actual apparent temperature of workpiece is less than 240 °C.

If the hot tool protrudes too far in front of the workpiece, the tool can be reflected in the workpiece.

Visible light image

Thermal image
Imaged temperature in °C

(a)

Turning marks in workpiece illuminated by hot chips make the workpiece appear to be about 300 °C.

Hot, flying chips may sometimes also be reflected.

Visible light image

Thermal image
Imaged temperature in °C

(b)

Both the optics and electronics of any camera system can introduce uncertainties in the images they produce. *Optical crosstalk* is unwanted scattering and reflections in the imaging system which causes intensity values of some pixels to apparently affect intensity values of other pixels. *Electronic crosstalk* is when the construction of the electrical circuitry within the FPA causes intensity values of some pixels to apparently affect intensity values of other pixels. Both optical crosstalk and electronic crosstalk are especially noticeable when there is a high ratio between the intensities of the brightest and darkest areas in the image. Figure 7 shows a simple experiment used to gauge optical and electronic pixel crosstalk.

Figure 7   A simple experiment used to gauge optical and electronic pixel crosstalk
(see online version for colours)
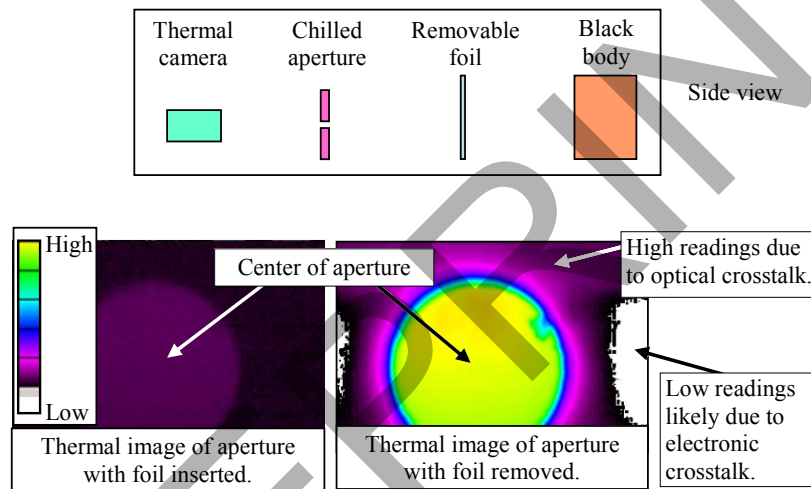
Note: Two images are compared, one with and one without a foil (acting like a shutter).

3.2   *Portion of camera response curve utilised*

In general, each pixel on an FPA has an 'S' shaped response curve, shown in Figure 8(a). The size and shape of the curve may be manipulated by adjusting the integration time or the optical filtering used. Figure 8(a) shows a situation with two desirable characteristics. First, only the linear range of the camera is used. Second, the entire linear range is used, not a small section of it. Figure 8(b) shows just the lower portion of the same curve. A *single point calibration* of a thermal image is when a single value for each pixel is used to correct the image. A single point calibration only corrects for errors in the offsets of the camera response at each pixel. This contrasts with a *two point calibration*, which uses a cold image and a hot image to correct both offset and slope errors. To remove both optically and electronically induced offsets, it is common practise to use a room temperature '*reference plate*' to perform a single point calibration. If the camera is used only in the linear portion of the response, then subtracting a constant (such as a reference plate reading) is a reasonable single point calibration.

Figure 8   Idealised camera response function (see online version for colours)
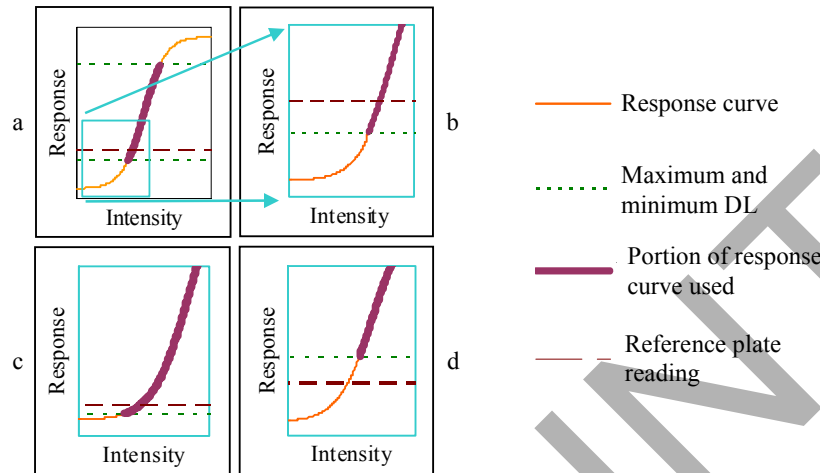
Note: Figure 8(a) and Figure 8(b) shows an ideal situation while Figure 8(c) and
       Figure 8(d) are problematic.

As shown in Figure 8(c), a researcher may wish to extend the dynamic range of the
camera by deliberately using the camera beyond the linear range. However, simple single
or double point calibrations may not be appropriate. This does not mean that the dynamic
range of the measurement cannot be extended by using both the linear and non-linear
portions of the response. It does mean that methodologies used when converting FPA
readings to temperature need re-evaluation.

Figure 8(d) shows another potentially problematic situation. Here, the camera is
operated within the linear range, but the reference plate is at too low a temperature
(intensity) and the measured digital reading is 0 (zero) DLs. All objects emit light due to
their temperature – even the optics of the camera system. Imagine a scenario where the
temperature of the optics increases or decreases, causing them to emit more or less light.
This causes the intensity of light received by the FPA while measuring the reference plate
to change. However, since the reference plate reading is below zero DLs, the camera only
reports zero and thus the change is not compensated for. This error may be avoided by
using a reference plate at a high enough temperature that the camera yields DLs above
zero.

Each pixel in the FPA has a different response. Thus, it is possible for some pixels to
be operating in the linear range [Figure 8(b)] while others are not [Figure 8(c) for
example]. When gauging whether the FPA is operating in the linear range, one has to
consider the responses of the individual pixels instead of the average response.

3.3   *Non-uniformity and calibration*

Each pixel on the FPA has a different sensitivity to light. Also, the amplifiers in the
analogue to digital converters in the FPA may have slightly different gains and offsets.
The resulting non-uniformity in response is especially evident at short integration times.
The process of correcting for these effects is called a non-uniformity correction, or *NUC*.

There are many schemes for performing a NUC. Some are quite complex, and it is not always obvious how they affect camera calibration.

One issue affecting which NUC procedure to use concerns whether the calibration and NUC of the system are viewed as two separate procedures or as one combined procedure. Figures 9 and 10 illustrate this. Since most thermal cameras have a field of view larger than the blackbody, off-the-shelf thermal camera software generally uses the two step method shown in Figure 9. Our system uses custom software which combines the NUC and calibration into one procedure, shown in Figure 10. A series of images of a blackbody is acquired at various blackbody temperatures. The blackbody is in focus and fills the field of view for the portion of the FPA used. For each pixel, a cubic spline describing temperature as a function of camera response is generated. Thus, each cubic spline will function as a calibration curve for that pixel. These are stored in a database. This process is repeated for each integration time used. After a cutting experiment has been performed, the software applies each calibration curve to the matching pixel for each frame in the movie. This converts the intensities in the thermal movie to imaged temperatures. Note that this procedure is applied offline, well after the data has been acquired. Also, note that most off-the-shelf thermal camera software assumes the camera is being used in the linear portion of the FPAs response. Our custom software allows for as many calibration points as desired, enabling operation in the non-linear portion of the FPA if needed.

Figure 9   When the in-focus field of view of the thermal image is larger than the calibration source, the NUC and calibration must be performed into two separate steps (see online version for colours)
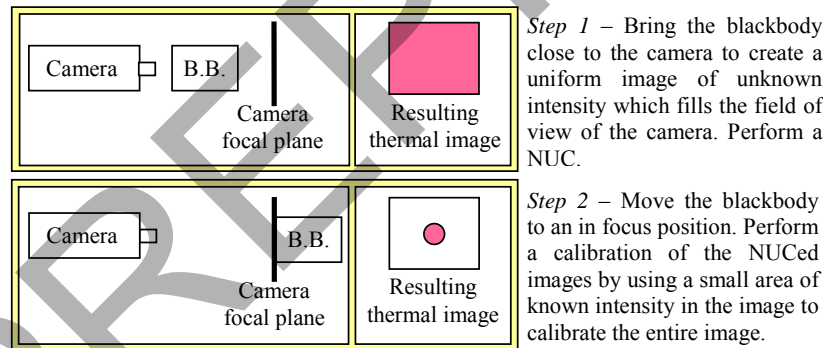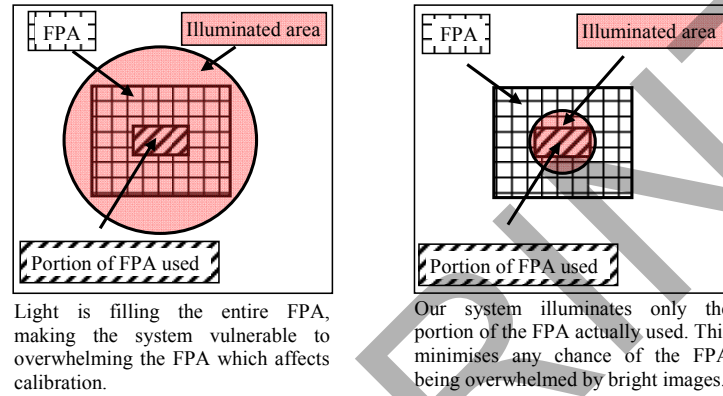

Step 1 – Bring the blackbody close to the camera to create a uniform image of unknown intensity which fills the field of view of the camera. Perform a NUC.

Step 2 – Move the blackbody to an in focus position. Perform a calibration of the NUCed images by using a small area of known intensity in the image to calibrate the entire image.

Figure 10   When the in-focus field of view of the thermal image is smaller than the calibration source, the NUC and calibration may be combined into one step (see online version for colours)

Since the intensity of this image is known and uniform, both the NUC and the calibration may be performed in one step.
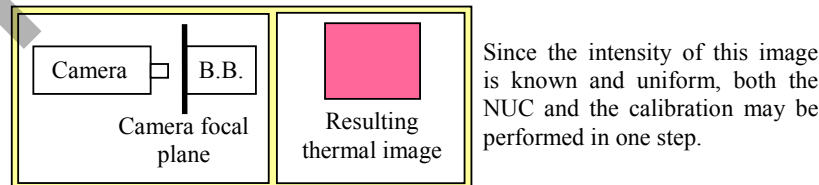
When filling the entire field of view with a blackbody image, one must be careful to not 'overwhelm' the FPA. The pixels of an FPA share a power supply through circuits with resistances. If all the pixels are simultaneously exposed to very bright light, the voltages supplied to the amplifiers on the FPA may drop, affecting the calibration. However, we do not use the entire FPA. As shown in Figure 11, our optics allow light to fall on only a portion of the FPA, avoiding this problem.

Figure 11 Avoiding the problem of overwhelming the FPA (see online version for colours)

Light is filling the entire FPA, making the system vulnerable to overwhelming the FPA which affects calibration.

Our system illuminates only the portion of the FPA actually used. This minimises any chance of the FPA being overwhelmed by bright images.

4   Converting imaged temperature to apparent temperature

In real-world situations, multiple uncertainty sources often act together to affect a measured value. When imaging the metal cutting process, some features of interest may be very small. For example, the thickness of the shear zone can range from 0.1 µm to 50 µm in size. A variety of factors makes measuring the temperatures of such small features problematic. One factor is that spatial resolution is limited by the wavelength of light used to image the feature. Visible light cameras are sensitive to wavelengths of less than 1 µm, while thermal cameras are sensitive to wavelengths up to 24 µm. This is the primary reason visible light cameras are generally able to image smaller features than thermal cameras. Also, if a feature is so small that it does not completely fill a pixel, the measured amplitude will be incorrect since a pixel measures average intensity over the pixel area. In addition, imperfections in the optics are more noticeable when imaging small features. One method for describing how the aforementioned effects influence the camera image is the PSF, which describes the response of an imaging system to a point source. It should be noted that diffraction effects are also possible, but are ignored in this analysis.

Figure 12 shows a one-dimensional model for the effects of the PSF and motion blur on the imaged intensity data. The undistorted, true intensity curve of the chip is modelled as a bar function (term A of the convolution) representing a shear zone of width W_{SZ} and intensity I_{SZ}, surrounded by a constant value I_{CF} representing the intensity of the chip faces. This curve is convoluted with the normalised PSF for the camera (term B) and a normalised bar of width W_{MB} representing the distance travelled by the shear zone during the integration time of the camera (term C). The area under both the PSF (term B) and the

motion blur curve (term C) is 1, so the area under the shear zone and chip face intensity curve (term A) is not altered by the convolution. However, the convolution will reduce the height and increase the width of the modelled shear zone intensity data.

In theory, if one knows the PSF and W_{MB}, they may be deconvolved from the measured intensity data to compute the shear zone and chip face intensity curve. However, there are two difficulties with this approach. First, deconvolution is very sensitive to noise in the data. Computed results vary wildly in response to even small changes in the input data. Second, the imaged intensity data is often an incomplete dataset due to the chip face being much cooler than the shear zone. In order to have enough sensitivity to measure the chip face temperature, the integration time must be increased. However, increasing the integration time also increases the motion blur. If the integration time is made too long, the motion blur can become so severe that the thermal image lacks sufficient detail. Thus, one often does not have data for the cooler portions of the measured intensity data.

An alternative approach is to select values for W_{SZ}, I_{SZ}, I_{CF}, W_{MB}, and the PSF. The convolution is computed and compared to the imaged intensity data. If there is good agreement, the selected values are plausible. One advantage to this approach is that sensitivity analysis may be performed. For example, if changing I_{SZ} by a large amount has little effect on how well the computed convolution matches the imaged data, uncertainty in I_{SZ} is large.

Figure 12   Schematic of modelling imaged intensity data as a convolution of the emitted intensity (term A), the camera PSF (term B), and motion blur (term C) (see online version for colours)
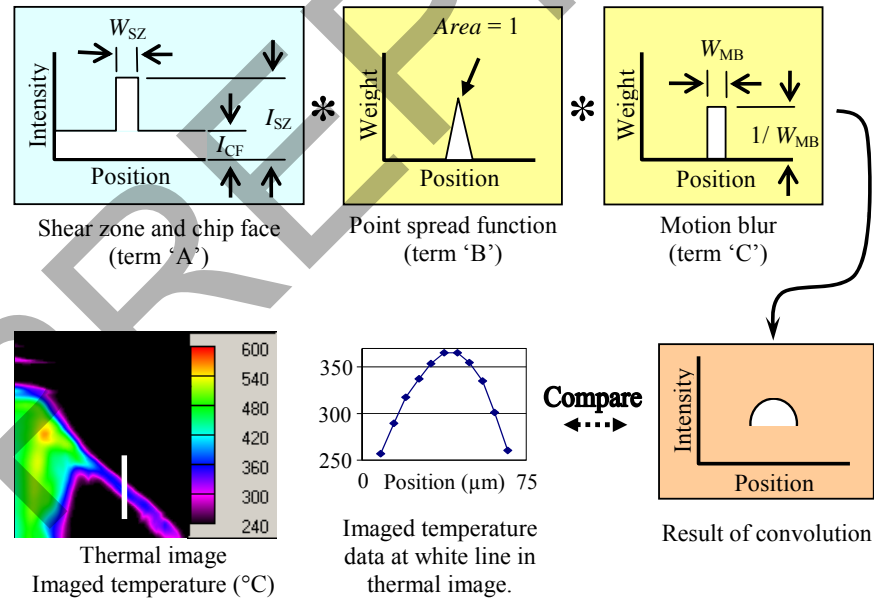

Note: Imaged temperature data may be converted to intensity and compared with the
        results of the convolution to determine if the input terms are reasonable.

Figure 12 shows a thermal image of segmented titanium chip formation we will analyse using this approach. The thermal camera was insensitive to temperatures lower than 240°C. The face of the chip is 240°C or cooler while the shear zone is over 350°C. To estimate W_{MB}, successive visible light images (not shown here) were examined. To create a one dimensional imaged intensity dataset, temperatures were sampled along a line through the shear zone in the thermal image. In addition to the data derived from Figure 12, the PSF for the camera was used. Procedures for determining the PSF are beyond the scope of this paper. Custom software allows a user to input values for W_{SZ} and the temperature which corresponds to I_{CF}. It then solves the convolution, setting the value of I_{SZ} so that the area under the computed convolution curve is equal to the area under the imaged intensity curve. The root mean square (*RMS*) value of the *residuals* (differences between imaged values and results of the convolution) is also generated.

It is interesting to note that the primary factor determining whether the computed convolution is a good fit to the measured image intensity (small RMS of the differences) is how well the overall widths of the two curves match. This is illustrated by the example shown in Figure 13.

Figure 13 Illustrative example showing that the lowest RMS of the residuals is obtained when the width of the measured image intensity curve matches the width of the resulting convolution (see online version for colours)
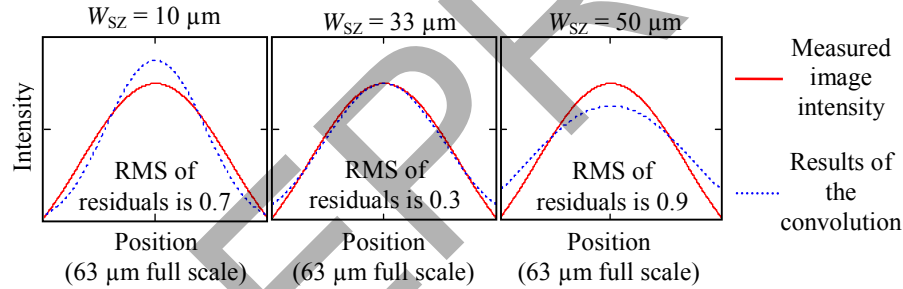
Note: $I_{CF} \cong 240°C$ and $W_{MB} = 29$ μm

In Figure 14, three values for W_{MB} are tried, 10 μm, 16.25 μm, and 22.5 μm. These values correspond to the measured value for W_{MB} as well as +1 thermal image pixel (+1.25 visible image pixel) and –1 thermal image pixel (–1.25 visible image pixel). It is assumed that we have measured W_{MB} to this level of accuracy. We assume I_{CF} corresponds to either 240°C or 130°C. $I_{CF} \cong 20°C$ was also tried and yielded results similar to 130°C, so results for 20°C are not shown. The grey horizontal line in Figure 14 is drawn at the height of the imaged shear zone temperature, 366°C. The range of likely T_{SZ}, the apparent temperature of the shear zone, is shown in the two gold coloured ovals. We can safely say that T_{SZ} is between 366°C and 384°C. Emissivity may be determined after the cutting test and used to convert this range into a range of plausible true temperatures for the shear zone.

Figure 14   Results where I_{CF} is assumed to correspond to either 130°C or 240°C, and W_{MB} is the measured value, the measured value +1 thermal image pixel, and the measured value −1 thermal image pixel (see online version for colours)
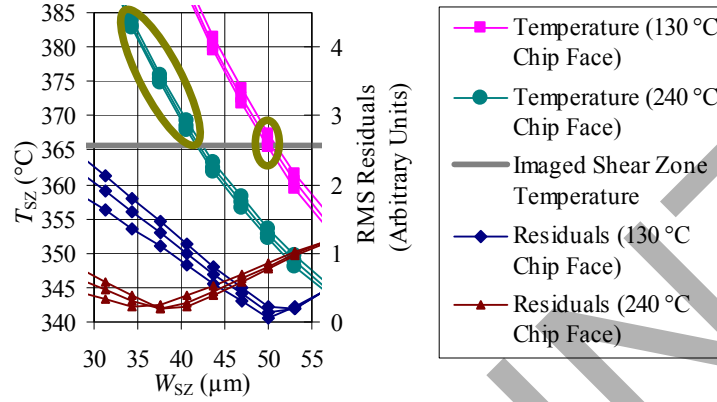
Note that if $I_{CF} \cong 240$°C, the narrower (34 μm to 41 μm), hotter (368°C to 384°C) shear zone values are more likely to be correct. If $I_{CF} \cong 130$°C, the wider (50 μm), cooler (366°C to 368°C) shear zone values are more likely. Knowing the chip face temperature is important information − even if the shear zone temperature is the ultimate goal. A repeat test, with the same cutting conditions but a long enough integration time to capture the chip face temperature, may be useful here. This example indicates that motion blur and PSF effects may be more accurately compensated for if other information, such as chip face temperature, is measured.

This example showed a titanium chip and had low uncertainty. This is in part due to the surface speed of the workpiece (and the chip) being relatively low. However, many materials are cut using much higher surface speeds. In these cases, the uncertainty is significantly worse due to increased motion blur. Also, this example showed a segmented chip. The location of the shear zone generally coincides with the location of the gap between segments. This has the effect of widening the shear zone. We are currently exploring unsegmented, continuous chips. It is suspected that continuous chips may have thinner shear zones. If this is the case, the uncertainty due to the PSF of the camera will be larger than in this example.

If the effects of imperfections in the image acquisition process are small, apparent and imaged temperature will be essentially the same, and the step of converting imaged temperature to apparent temperature may be skipped.

5   Converting apparent temperature to true temperature

5.1   *Factors to consider*

5.1.1   *Features being measured*

Generally, a machining researcher is most interested in the temperature of certain features and less concerned with other features. Potential interesting features include the workpiece, the shear zone, the chip, the body of the cutting tool, and the interface

between the rake face and chip. Each presents a unique set of measurement issues to consider, and requires a different level of effort. It is often difficult to accurately measure more than one feature at once. For example, if the side of the tool is in focus, the workpiece might not be in focus. An integration time which is long enough to capture the cooler workpiece temperatures may result in the details of the rapidly moving hot chips being motion blurred beyond usability. Several examples are discussed next.

- *The body of the cutting tool:* Several factors result in a properly prepared tool (see Section 5.2.1) being the easiest to measure. The emissivity has a relatively constant value. The emissivity also has a relatively high value, and the tool is generally hot, so reflections are less of a concern. The side of the tool is relatively flat, so depth of focus is not an issue. Perhaps the most difficult issue confronted when imaging the side of the tool is determining the precise location of the edge of the tool. Compared to the workpiece or chip, the tool is relatively motionless, so motion blur is less of an issue. However, cutting forces often induce tool motion due to static deflection or vibration. The long wavelengths of thermal images result in images which do not have a high spatial resolution, resulting in images without sharp detail. Additional factors include reflections of the chip in the rake face and sideflow of the chip. All these factors can result in the tool edge being a challenge to precisely locate.

- *The workpiece:* As illustrated in Figure 6, reflections are often the greatest challenge when measuring workpiece temperatures. While the workpiece is moving rapidly, motion blur is acceptable if the emissivity of the surface is reasonably uniform and one is concerned only with average trends in workpiece heating.

- *The interface between the rake face and chip:* As illustrated in Figure 3, knowing the emissivity of the interface is problematic. Also, there is the potential for the light emitted by the chip to reflect off of the rake face of the tool and adversely affect the temperature readings of the interface.

- *The chip and the shear zone:* Chip temperature is probably the most difficult to measure. Side flow of the chip can make the small depth of focus a significant issue. As discussed in Section 4, high chip velocity, combined with very non-uniform temperatures, is a challenge. Section 5.2.2 discusses the additional challenge of highly variable emissivity.

5.1.2 *Type of quantity being measured*

When compared to an average temperature, the peak temperature has the advantage that it is easy to locate; just pick the highest value in the image. However, if the size of the 'hot spot' is small, the amplitude of the peak can appear low due to effects such as the PSF (see Section 4). This contrasts with the average temperature over a larger area, which is generally less susceptible to size of source effects. However, if the image is significantly motion blurred and the imaged object has a wide range of temperatures and emissivities, the measured 'average' temperature can be inaccurate (see Section 5.2.2). A second issue to address when determining an average temperature is that one typically does not want the average of the entire image. Instead, one typically wants the average of some region of interest, for example, a 50 μm by 50 μm area centred 100 μm from the edge of the tool. The challenge then becomes one of accurately locating the region of interest so the pixels to include in the average may be determined.

5.1.3 Form of the equation used to convert apparent temperature to true temperature

The conversion of apparent temperature to true temperature is based on Planck's equation. Planck's equation describes the radiance of a black body at a certain wavelength as a function of the true temperature. There are multiple modifications of Planck's equation in the literature. Some take into account effects such as reflectivity, transmittance, atmospheric absorption, multiple reflections, changes in emissivity as a function of temperature, or whether to use a single wavelength or integrate over a range of wavelengths. The characteristics of the camera system and of the scene being imaged must be considered to decide which form is best.
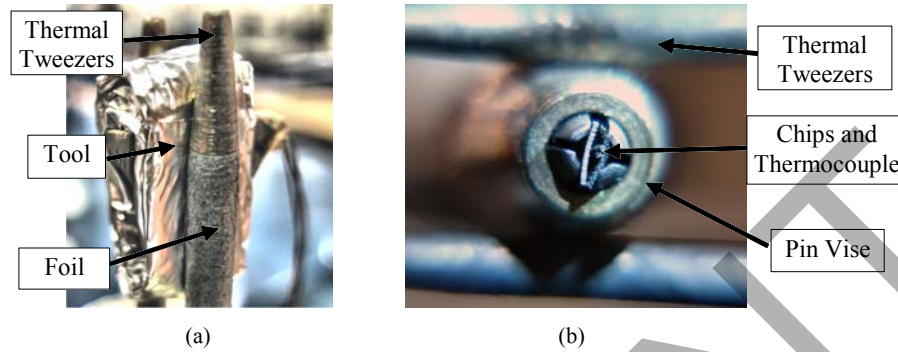
5.2 Emissivity

Handbook values for emissivity are available for many materials. However, most materials have a different emissivity value at each wavelength of light, as well as a different emissivity value at each temperature. Handbook values do not always specify the wavelength and temperature range over which the stated emissivity value is valid. Emissivity is also strongly affected by factors such as surface texture and oxide layers. The surface texture and oxide layers of the workpiece material change dramatically as it is transformed into a chip during the machining operation. Thus, emissivity of workpiece material changes significantly during machining. Also, handbook values are generally acquired under ideal conditions using an integrating hemisphere. An *integrating hemisphere* is a device which efficiently captures nearly all of the thermal spectrum radiation emitted by a surface in all directions. A real world camera can only capture a portion of the radiation emitted. The end result is that handbook values are often of little use, and emissivity of the surface should be measured whenever possible.

One way of measuring emissivity is to heat the surface to a known temperature and image it with the same thermal camera used to image machining. The difference between the apparent temperature and known temperature may be used to compute emissivity. However, this assumes there are no reflections on the surface from thermal radiation emitted by other hot objects. Thus, one cannot simply image the object inside a hot oven, since the hot sides of the oven may be reflected off the surface of the object. Two examples will be shown next.

5.2.1 The cutting tool

Figure 15(a) shows a tool temporarily wrapped in aluminium foil and heated by thermal tweezers. The foil is wrapped in such a way that the surface being imaged by the thermal camera does not have any thermal radiation emitted by the hot foil reflected off the surface. A thermocouple in contact with the tool measures its true temperature. Comparing the thermal image to the true temperature of the tool allows the emissivity to be computed.

Figure 15 Objects may be heated to known temperatures and imaged with a thermal camera, (a) measuring the tool (b) measuring the chip (see online version for colours)


<div align="center">(a)   (b)</div>

Note: Comparing the apparent temperature to the true temperature may be used to estimate their emissivity.

In theory, one could perform this procedure either before or after the machining experiment. However, machining generally heats the tool to high temperatures which may cause oxide layers to form. This results in a constantly changing emissivity of the tool during machining. Thus, this procedure should be performed before the machining test so the tool may be 'pre-oxidized'. This minimises changes in emissivity during machining experiments. Note that before one acquires the thermal images used to determine emissivity, one should hold the tool at the elevated temperature for a sufficiently long period to enable the oxide layer to fully develop.

5.2.2 The chip

To measure the emissivity of the side of the chips imaged during machining, two chips are placed in a pin vice with a thermocouple sandwiched between them. Shown in Figure 15(b), thermal tweezers are then used to heat the chips to a known temperature. The chips are imaged by the dual spectrum system and the difference between the thermocouple and apparent temperature is attributed to local emissivity of the chip surface. Due to the extreme deformation involved, chips typically have a much rougher surface than the workpiece. One expects the chips to be more emissive than the workpiece due to this dramatic increase in surface roughness. Figure 16 shows a visible and thermal spectrum image of a segmented chip. The area of the chip with side flow is often out of focus due to the limited depth of field of the camera system. Emissivity $\varepsilon \approx 0.3$ for the segment faces while $\varepsilon \approx 0.5$ for the segment gap and side flow portions of the image. It is not uncommon for emissivity values to vary from 0.2 to 0.6 on a single segment face. With such a large variation in emissivity, a large temperature uncertainty is difficult to avoid.

Figure 16   A visible and thermal spectrum images of a segmented chip with corresponding
                  emissivity values (see online version for colours)
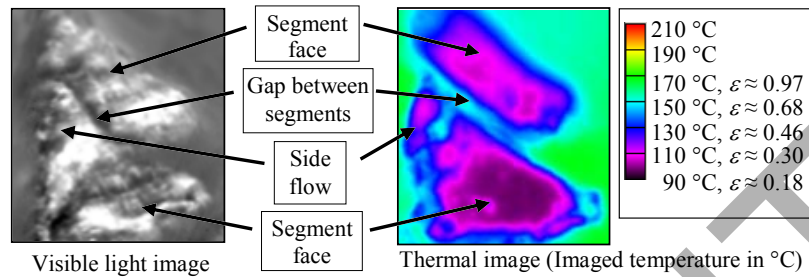

Notes: Imaged temperature is assumed to be approximately equal to apparent
       temperature. The 172°C chip is about 0.6 mm thick (left to right in the image).

Some researchers attempt to avoid the issue of non-uniformity by using a very long integration time while imaging chip formation. During a long integration time, chip motion causes different portions of the rapidly moving chips to be projected onto any given pixel. When the chips are segmented, there are two types of portions, faces of the chips and gaps between the segments. Assuming a perfect camera, each portion has an instantaneous intensity which is determined by the true temperature and emissivity of that portion. At the end of the integration time, the average of these instantaneous intensities is what the camera has measured for that pixel. However, while each pixel may represent an average intensity, it does not necessarily yield an average (arithmetic mean) temperature. This is because the equation converting intensity to temperature is highly non-linear. The resulting uncertainty is significant if the temperatures and emissivities of the chip surface are highly non-uniform. Segmented chips are more likely to be affected by this than continuous chips, which are relatively uniform.

When measuring emissivity of the chip after a machining test, the researcher should be aware that the emissivity of the chip after machining may not be the same as it was during machining. This is due to the fact that an oxide layer continues to build on the hot chips well after they have exited the field of view of the camera. Figure 17 illustrates that oxidation is a reaction that takes time to occur. The two images, acquired from two different vantage points at the same moment in time, show a very thin chip that, as it emerges from the tool, is not hot enough to visibly glow. Further down the chip, several milliseconds have past since this portion of the chip has been cut, yet it is hot enough to glow very brightly. The once solid chip sometimes melts and boils well after the test is finished. In this case, oxidation is an *exothermic* (produces heat) process. The reason the temperature rise is not obvious with normal, thicker chips is that thick chips have a lot more metal to absorb the exothermic heat energy. That is, thick chips have a higher volume to surface area ratio. It should be noted that oxidation is not always exothermic. Other workpiece materials may be *endothermic* (receives heat from the surroundings) or temperature neutral. There may also be some *superheating* of the material during cutting (being heated above the melting temperature but not having time to transform from a solid to a liquid). However, well after the chips have left the cutting zone, they glow dramatically brighter than what may be attributed to any emissivity changes alone. Thus, it is likely that an exothermic reaction is the dominant cause for the behaviour shown in Figure 17.

Figure 17   A very thin steel chip, less than 0.1 mm thick, illustrating exothermic oxide formation (see online version for colours)

Camcorder image   Low-magnification grey scale
                                   Visible light image
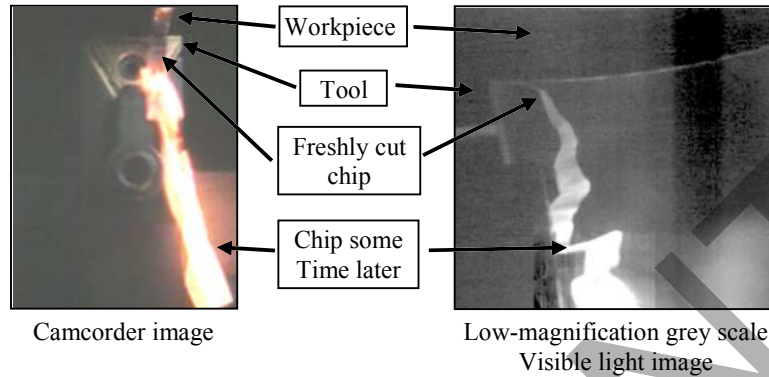
6   Conclusions

This paper introduces the machining researcher to many of the concepts needed to navigate the challenging task of acquiring and interpreting thermal images of machining. With this understanding, thermal images may be correctly interpreted and used to improve our knowledge of the machining process.

Disclaimer

This document is an official contribution of the National Institute of Standards and Technology and is not subject to copyright in the USA. The National Institute of Standards and Technology does not recommend or endorse commercial equipment or materials, nor does it imply that the equipment or materials shown are necessarily the best available for the purpose.

Acknowledgements

References

Baer, R.L. (2003) 'Circular-edge spatial frequency response test', *SPIE Proceedings*, Vol. 5294, pp.71–79.

Boreman, G.D. and Yang, S. (1995) 'Modulation transfer function measurement using three- and four-bar targets', *Applied Optics*, Vol. 34, No. 34, pp.8050–8052.

Davies, M.A., Ueda, T., M'Saoubi, R., Mullany, B. and Cooke, A.L. (2007) 'On the measurement of temperature in material removal processes', *CIRP Annals – Manufacturing Technology*, Vol. 56, No. 2, pp.581–604.

Holst, G.C. (2003) *Holst's Practical Guide to Electro-Optical Systems*, JCD Publishing, Winter Park, FL, available at http://www.jcdpublishing.com/book8.html.

Ivester, R.W. and Heigel, J.C. (2007) *Smart Machining Systems: Robust Optimization and Adaptive Control Optimization for Turning Operations*, Transactions of the North American Research Institute (NAMRI)/SME, Vol. 35, pp.505–511, available at http://www.nist.gov/customcf/ get_pdf.cfm?pub_id=822723 (accessed on 23 January 2012).

Longbottom, J.M. and Lanham, J.D. (2005) 'Cutting temperature measurement while machining – a review', *Aircraft Engineering and Aerospace Technology: An International Journal*, Vol. 77, No. 2, pp.122–130.

Nill, N.B. (2001) 'Conversion between sine wave and square wave spatial frequency response of an imaging system', MITRE Technical Report MTR01B0000021.

Whitenton, E.P. (2010a) 'High-speed and dual-spectrum videos of machining processes', available at http://www.nist.gov/el/isd/sbm/hsds-machining-videos.cfm (accessed on 23 January 2012).

Whitenton, E.P. (2010b) *High-Speed Dual-Spectrum Imaging for the Measurement of Metal Cutting Temperatures*, National Institute of Standards and Technology, NISTIR 7650, available at http://www.nist.gov/manuscript-publication-search.cfm?pub_id=904301 (accessed on 23 January 2012).

Zhang, Z.M., Tsai, B.K. and Machin, G. (2010) *Radiometric Temperature Measurements: II. Applications*, Elsevier Academic Press, New York, NY.